Proceedings of ASME Turbo Expo 2019: Turbomachinery Technical Conference and Exposition
GT2019
June17-21, 2019, Phoenix, Arizona, USA

GT2019-91629

AN EXPERIMENTAL STUDY OF PASSAGE-TO-PASSAGE FLOW INTERACTIONS IN A SINGLE STAGE AXIAL FLOW RESEARCH TURBINE ROTOR

Veerandra C. Andichamy and **Cengiz Camci**
The Pennsylvania State University, Dept. of Aerospace Engineering
Turbomachinery Aero-Heat Transfer Laboratory
University Park, PA, 16802

Yong W. Kim
Aero/Thermal and Performance Department
Solar Turbines Inc, 2200 Pacific Hwy
San Diego, CA, 92186

ABSTRACT

During the lifetime of a turbine stage, some of the blade tips may undergo changes due to mechanical rubbing with casing surface and also due to thermal oxidation. Understanding the effect these damaged blades have over the undamaged blades is essential to estimate the performance of the turbine stage in the operable tip clearance range. In this paper, the passage to passage aerodynamic interaction in a turbine stage is studied by modifying the tip gap of selected turbine blades and analyzing their effect on the neighboring blade passage flows. The experiments in this study are carried out in a single-stage low-speed axial turbine facility. All measurements are taken in the stationary frame of reference using a time-accurate differential dynamic pressure transducer mounted in a Kiel probe head. The experimental results from this study show that even with a significant increase on a selected blade's tip clearance, its effect on the AFTRF turbine flow is only confined to its neighboring blade passage. The disturbances due to the altered tip clearance of one passage are not measurably propagated to its neighboring turbine passages. The changes made in one of the blades in a turbine stage do not significantly alter the aerodynamic performance of other blades. This result is particularly important for large-scale turbine research rigs such as AFTRF where the unsteady total pressure field is mapped in a time-efficient and phase-locked manner.

NOMENCLATURE

AFTRF	Axial Flow Turbine Research Facility
C_p	Total pressure coefficient, $C_p=\Delta P_0/0.5\rho U_m^2$
Delta C_p	Delta C_p= [C_p - (*reference* C_p]
DTP	Dynamic Total Pressure (probe)
h	Rotor blade height, h = 0.123 m
H	Relative span-wise location, measured from rotor hub, normalized by L
HP	High Pressure
L	Passage height, L = h+t
N	Rotor speed (RPM)
NGV	Nozzle Guide Vane
P_{atm}	Atmospheric pressure, typically P_{atm} = 97,800 Pa
ΔP	Pressure difference measured by Validyne transducer
ΔP_0	Total pressure difference measured by DTP probe
r_m	Rotor radius at mid-span, r_m = 0.3923 m
SLA	Stereo-lithography based additive manufacturing
t	Rotor tip clearance height
T_o	Total temperature
TC	Relative tip clearance, TC = t/h
U_m	Mid-span rotor speed, $U_m = \omega.r_m$
α_3	Rotor exit absolute flow direction from axial direction
δC_p	Uncertainty of C_p, $\delta C_p = \pm 0.39\%$
ρ	Density of the flow
ω	Angular velocity of the rotor blade

INTRODUCTION

Due to the severe aero-thermal and highly rotational environment of a gas turbine rotor, the blades operate in an extreme environment where they experience unusually high temperatures, thermal stress, mechanical stress, oxidation, and fatigue. This is especially true for blade tips, as there is a good possibility of mechanical rubbing with the casing surface.

Tip leakage flows further complicates the thermal problem near the tip gap as it brings hot mainstream gases into this region. This increases the local temperature and induces

additional heat flow to tip surfaces, Mayle et al. [1]. The trailing edge of the blade tips and the pressure side tip corner are possibly the most affected zones due to its wedge-shaped structure. Bindon et al. [2] showed that because of tip leakage flows, a phenomenon called tip-burnout may occur where blade tips may melt due to increased thermal loads.

During the operation of a turbine stage, there are several conditions which cause the reduction of blade tip gap, resulting in rubbing of blade tips against the casing surface. During transient operations, sudden change in temperatures could enhance the radial growth of the blades resulting in rubbing. This is especially true during engine start-up, and when the thermal response of the rotor assembly is slower than that of the stationary components, as shown by Evans et al. [3]. Rich et al. [4] showed that the casing surface also undergoes changes during the turbine operation which can cause a reduction in tip clearance gap. The non-uniform temperature distribution of the NGV inlet flow from the combustor distorts the casing surface, thus increasing the risk of rubbing.

A blade damaged either due to thermal oxidation or mechanical rubbing results in performance loss. This loss can sometimes be propagated to other undamaged blades in the same turbine stage. In a compressor environment, even a small change in the blade tip clearance results in a significant performance loss as shown by Ian [5] and also these effects are also propagated to the entire stage as seen by Ramakrishna et al. [6]. In a turbine stage, there is no significant circumferential flow propagation. But the extent to which one blade interacts with the others in a turbine stage has not yet been fully understood. The existing literature in this area is scarce. This interaction in a large-scale research turbine environment such as The Axial Flow Turbine Research Facility (AFTRF) is particularly important and it has never been studied. This paper culminated from the fact that tip clearance variations in the current 29 bladed AFTRF rotor operation can be significant because of specific tip clearance research requirements.

In an experimental turbine research rig such as the AFTRF, a blade tip can be modified with different tip designs without dis-assembling the whole rotor as shown in Fig. 1. Ideally, to investigate a novel blade tip design for aerothermal performance improvements, all of the blades in a rotor have to be modified with the same blade tip design. This approach dramatically increases the overall cost and time duration of the project. In order to perform fast and cost-effective research and development studies, one can modify only a few blades for the novel concept under investigation. The idea of having slightly altered blade passages, especially near the tip area may generate circumferential flow non-uniformity. However, our current investigation clearly shows that the propagation of the influence of the altered blade passages is not that significant. With the recent developments in the response time of the fast response thermal and pressure sensors, each individual blade passage can be aerodynamically analyzed during an experimental run, as explained by Andichamy, Camci and Khokhar [7], and Town [8, and 9]. The four subsequent blades carrying the novel tip design manufactured using an additive manufacturing technique (SLA) is shown in Fig. 1. Although Fig.1 shows the baseline tip geometry where the tip is a perfect cylindrical surface, any new tip design including squealer tips, partial squealers, pressure side extensions or other possible novel concepts can be installed in an extremely short amount of time in a cost-effective way. High-resolution additive manufacturing and careful dynamic balancing are the two key elements of the specific approach taken in this study. A time-accurate and phase-locked total pressure measurement of the rotor exit field is required for the simultaneous mapping of each blade passage in this effort. The current investigation clearly shows that modifying a few blades for an exploratory tip development effort does not generate significant circumferential non-uniformity issues in the large-scale turbine research rig AFTRF. The approach is highly cost-effective and time efficient. Fig. 1.a shows three subsequent turbine blade tip sections that are additively manufactured out of an SLA plastic material, ACURA-25. The SLA based tip manufacturing process involves turning a three-dimensional computer design drawing into a solid object through a rapid, repeated solidification of liquid resin. The computer file is digitally "sliced" into horizontal cross-sections of about 0.002″ (0.05 mm) thick. These "slices" are entered into a stereolithography prototyping machine where an ultraviolet laser traces and solidifies the tip section out of photo-sensitive polymer. The EDM cut metallic AFTRF blade tips and their SLA replacements for novel tip shape development for turbine tip leakage mitigation research are shown in Figure 1.b

Any modification made near the tip section of a turbine blade can be seen in its own blade passage, as shown by Andichamy [10]. Hence, by carefully analyzing the individual passage flows simultaneously, the overall aerodynamic changes occurring because of the installation of novel blade tip designs can be identified. The turbine passage has a highly complex flow field with different types of flow structures from core flow to airfoil boundary layers, from wake to secondary flows, from tip leakage flow to rim-seal flow contributions. These flow structures constantly interact with each other to create a highly 3D, unsteady and turbulent flow field. There has not been a comprehensive study to understand whether the influence of the tip gap modifications are limited to the altered passage or the influence of the altered tip gap is propagated to nearby passages in the same turbine rotor. In this study, the blade tips are modified by increasing their tip clearance value, and the influence of this change over other unmodified blades is studied by analyzing their individual passage flow patterns. The goal of this study is to understand the effect the modified blades representing the novel tip design over the performance of other unmodified blades in the large-scale research turbine AFTRF.

EXPERIMENTAL FACILITY AND PROCEDURE

Turbine Research Facility: The experimental data needed to study the interaction between different passages is collected in the Axial Flow Turbine Research Facility (AFTRF) as shown in Fig. 2. The AFTRF is an open-circuit large-scale turbine rig with an advanced axial turbine blade configuration. The research

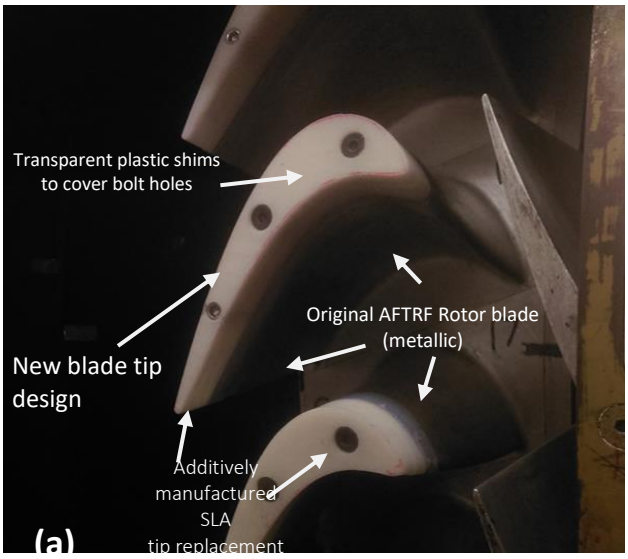

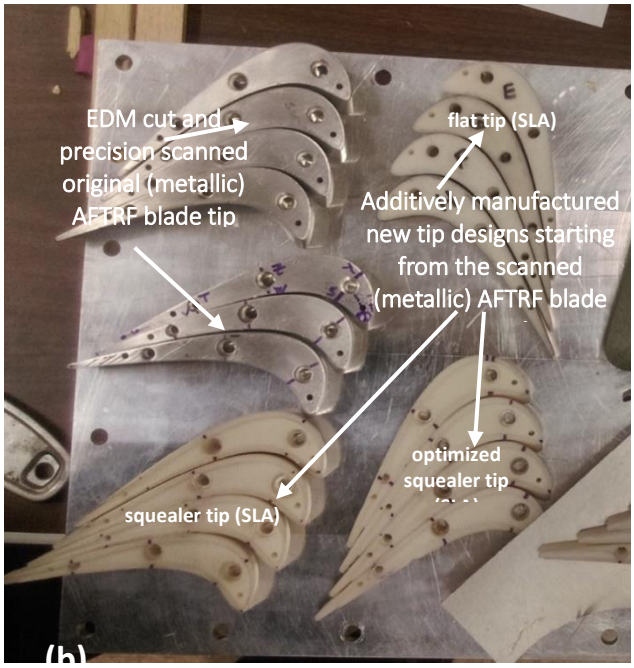

Figure 1: (a) Select turbine blades with different tip designs, additively manufactured four blade tips (white) out of SLA material,
(b) EDM cut metallic blade tips and their SLA replacements for novel tip shape development for turbine blade tip leakage mitigation

turbine is of cold flow type with atmospheric inlet temperature. The bell-mouth type inlet of the facility is followed by the test section containing a single HP turbine stage. Four-stage axial flow fans with adjustable pitch, connected in series are used to drive the turbine stage in the suction-blower mode. Around 80 HP of power is generated by the rotor assembly with a typical temperature drop of $5 - 7\,^0$C across the turbine stage. The power generated is absorbed by an Eddy Current Brake (ECB). The rotor RPM in the turbine stage can be controlled using this water cooled ECB and within ±1 RPM. A comprehensive report on this facility is given by Lakshminarayana, Camci, Halliwell, Zaccaria [11] and Town [8].

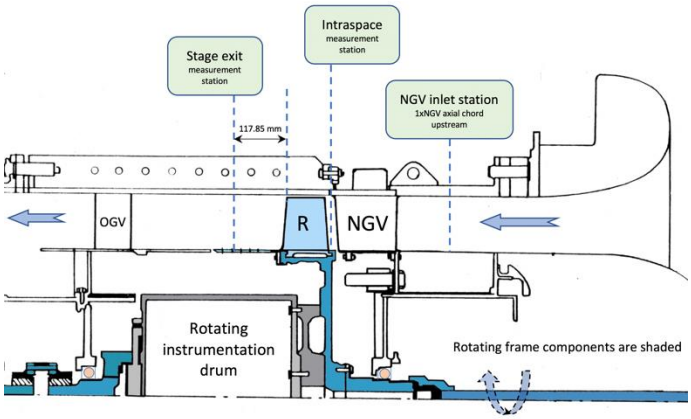

Figure 2: Cross-sectional drawing of AFTRF

The turbine stage has 23 Nozzle Guide Vanes and 29 rotor blades. Table 1 summarizes the main design features of the stator and rotor blades in the stage. The inlet characteristics of the flow entering the NGV is given by Town [8]. The Reynolds number of the flow based on the nozzle exit velocity and axial chord is in the range of 900,000 to 1,000,000. For the rotor, the Reynolds number calculated using the relative inlet velocity is in the range of 250,000 to 450,000. The Reynolds numbers in the turbine stage are representative of a modern HP turbine stage, as shown in Town and Camci [9]. The rotor blades have a span of h=123 mm with the hub to tip ratio of 0.732. In the absolute reference frame, the flow exits the rotor blade tip at an angle of 25.16^0 with respect to the axial direction. The rotor blades are named 1 to 29 and the current tip clearance measurement (static) of all the blades are present in Table 2. Due to the relatively low rotational speed of 1330 RPM, the static and run-time tip clearances are considered to be identical.

Instrumentation: The stagnation temperature at the NGV inlet and rotor exit are measured by K-type thermocouples. Pitot pressure probes measure the velocity of the flow at NGV inlet and rotor exit. Unsteady and phase-locked total pressure at rotor exit is measured by the Dynamic Total Pressure Probe (DTP) in a KIEL probe arrangement. DTP is in the stationary frame and located at 29.4% axial chord (25.4 mm) downstream of the rotor exit as shown in Fig. 3. The DTP probe is mounted at an angle of 25.5^0 with respect to the axial direction. On analyzing the sensitivity of DTP probe to yaw and pitch angle, Rao et al. [15] and Town [8] experimentally showed that this square cut probe design is insensitive to pitch/yaw angle variation within the uncertainty estimate of $\delta C_p = \pm 0.017$. Since the probe is especially aligned with the exit flow at blade tip, the pitch/yaw angle variations of the exit flow are unlikely to cause significant error as explained in the Appendix.

Table 1: Design features of AFTRF turbine stage

Parameters	Stator	Rotor
Number of blades	23	29
Zweifel coefficient	0.7247	0.9759
Tip relative mach number	---	0.24
Blade height (m)	---	0.1229
Turning angle, tip/hub	70^o	95.42^o / 125.69^o
Chord length (m)	0.1768	0.1287
Axial tip chord (m)	---	0.084
Spacing (m)	0.1308	0.1028
Maximum thickness (mm)	38.81	22

Table 2: The tip clearance values of all the blades

Blade No	Tip clearance (%) (t/h)	Blade No	Tip clearance (%) (t/h)	Blade No	Tip clearance (%) (t/h)
1	0.79	**12**	0.81	**23**	0.66
2	0.79	**13**	0.85	**24**	0.81
3	0.78	**14**	0.86	**25**	0.73
4	0.81	**15**	0.80	**26**	0.87
5	0.73	**16**	0.79	**27**	0.71
6	0.75	**17**	0.80	**28**	0.84
7	0.74	**18**	0.79	**29**	0.69
8	0.76	**19**	0.83		
9	0.80	**20**	0.81		
10	0.81	**21**	0.87		
11	0.81	**22**	0.69		

Table 3: The measurement uncertainty estimates

Parameter	Nominal Value	Uncertainty	Uncertainty (% of nominal value)
Validyne transducer, ΔP	7500 Pa	±5 Pa	±0.067%
Total pressure coefficient, C_p	4.42	± 0.017	±0.39%
K-type thermocouple, T	300 K	±1.0K	±0.333%
Rotor speed, N	1330 rpm	±1 rpm	±0.075%
Atmospheric pressure, P_{amp}	98700 Pa	±100 Pa	±0.101%
Tip clearance, t	1524 µm	63.5 µm	4.17%

The Unsteady DTP probe: The DTP probe has a flush-mounted differential dynamic pressure transducer with a reference port open to atmosphere. The transducer has a piezo-resistive sensor (Endevco 8507C-1) with a reported accuracy of 1.5% and time response of 18 microseconds making it effective in mapping the unsteady pressure field at the rotor exit. Detailed information of this unsteady aerodynamic probe is given by Town [8]. The DTP probe is moved radially in the measurement plane using the linear probe traversing system. The probe traversing system consists of a fast stepper motor (Vexta), a micro-stepper controller (Velmex VXM) and a linear traverser (Velmex Unislide). With the micro-stepping ability of the motor and its fast response, the probe can be placed at a desired location with great positional accuracy in a small amount of time. The linear traverser is mounted on the precision built and non-intrusive window. The BEI-Sensors optical encoder attached to the turbine shaft measures the RPM of the rotor. The encoder also provides 6000 measurement bins per revolution.

Phase-locked Data Acquisition: The experimental flow properties and rotor performance are measured and calculated instantly and displayed on a LABVIEW GUI screen. The dynamic total pressure data measured by the DTP probe is phase-locked to the rotor with the help of the optical encoder. As the encoder is directly attached to the turbine shaft, it ensures that the data obtained by the DTP probe is phase-locked with the rotor even if there is any slight change in the rotor RPM. A detailed description of the data acquisition used in this study is given by Andichamy in [10].

In the current experiment, the DTP probe is moved radially from H=97% blade-span to 25% blade-span with an increment of 1% blade-span. The data from the hub (H = 0.0) to (H = 0.25) are not measured for time savings since the current research is towards tip region measurements. The data from the outer casing (H = 1.0) to (H = 0.97) are also not considered due to the DTP's wall proximity character and safety concerns. At a selected radial position, the DTP probe always collects 6000 phase-locked total pressure measurements per revolution. To obtain statistically stable results, at each radial position the DTP probe collects data for 400 subsequent revolutions. An ensemble averaging is applied over 400 revolutions instantly.

Experimental Uncertainty: The measurement uncertainties (based on a 95 % confidence interval) of the various sensors used in this study are given in Table 3. The uncertainties are evaluated by the approach presented by Kline and McClintock [12]. Further details of the measurement system are given by Dey, Rao, Gumusel, Town, Akturk, and Camci in [9, 13, 14, 15 and 16].

Design of Experiments: To understand the interaction between the passages in a turbine stage, two experiments (Test 1 and Test 2) are performed on the AFTRF facility.

Test 1: In Test 1, all of the blades are in the typical tip clearance range of t/h=0.66% to t/h=0.87%. Exact tip clearance values of all 29 blades are shown in Table 2. The tip clearance value is measured individually using a precision filler gauge when the rotor is stationary. The running clearances of the blades are assumed to be similar to the stationary clearance, as the large-scale cold turbine rig runs at a low speed of 1330 RPM. There is

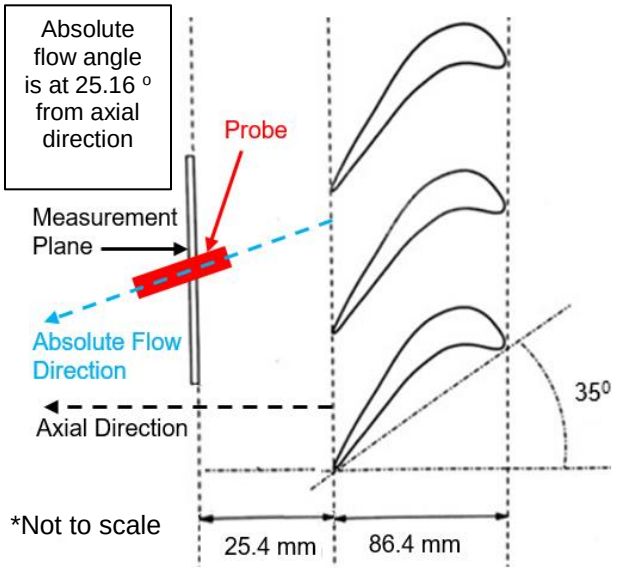

Figure 3: Measurement arrangement at the rotor exit, [7]

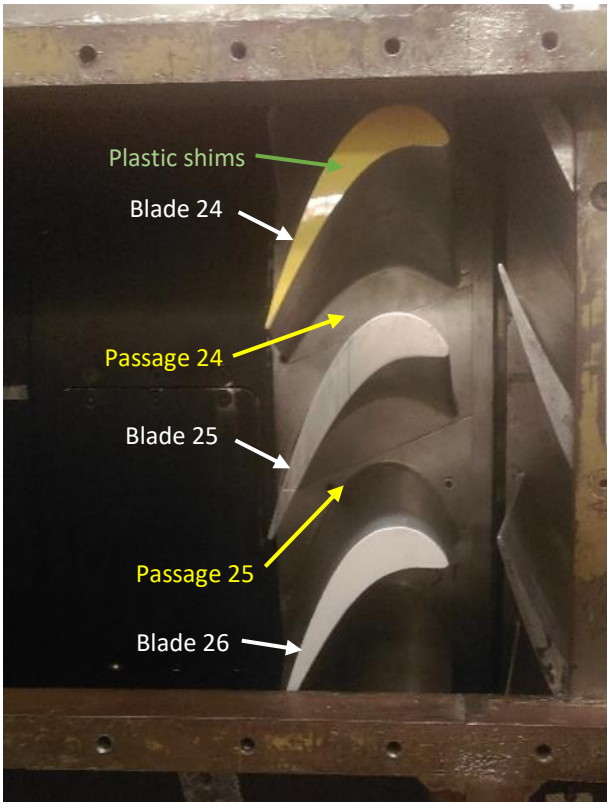

Figure 4: Blades and their corresponding passages

not enough centrifugal force to distort/elongate the rotor blades. The thermal distortions are also minimal since the facility operates near ambient temperature conditions. The convention is that the passage on the pressure side of a given blade has the same name as the blade as indicated in Fig. 4. With the phase-locked DTP probe measurement, the aerodynamic character of each blade passage can be easily identified and correlated with its tip clearance value in a 20 minute long single AFTRF run. The two blades, blade 24 and blade 26 are selected as the test blades for this study.

Test 2: In this experiment, the tip clearance of blade 24 is varied from 0.81% to 1.13% and similarly the tip clearance of blade 26 is varied from 0.87% to 1.34%, while all other blades remain same as shown in Table 2. The blade tip clearance can be varied by adding or removing thermo-plastic shims on the blade tip as shown in Fig. 4. The plastic shims in the shape of the blade tip airfoil are attached using heat resistant double-sided tape. On studying these two experiments the aerodynamic influence of the test blades 24 and 26 onto their neighboring blades can be observed. Only two blades are modified out of 29 blades, this was done mainly to study whether the effect of these variations is localized or global in the turbine stage. A detailed analysis of the effect these modifications in the passages 24 and 25 are presented. The impact of the relatively larger clearances of the blades 24 and 26 on their neighboring passages are also discussed in detail.

EXPERIMENTAL RESULTS AND DISCUSSION

The ensemble-averaged time-accurate total pressure data at three different blade-spans for Test1 and Test 2 have been non-dimensionalized as pressure coefficient C_p and presented in Fig. 5. The non-dimensional C_p values are calculated as follows.

$$C_p = \frac{\Delta P_{measured}}{\frac{1}{2}\rho U_m^2} \quad \textbf{(1)}$$

The numerator of Eq. (1) is the differential total pressure with respect to the atmospheric pressure, obtained from the DTP probe in the laboratory frame of reference.

Focus Areas and Rotor Arrangement: The three different blade-spans of H = 0.91, H = 0.53 and H = 0.25 have been strategically chosen, as they represent certain flow feature in the turbine flow field.

Tip leakage zone: At H = 0.91, the core of the leakage vortex is present indicating the region with the most influenced region from the tip leakage flow. Some interaction with the secondary flow zone underneath is very much likely in this area.

Mid-span: The core flow with a minimal tip leakage/secondary flow and end-wall boundary layer influence is present at mid-span, H = 0.53, representing the turbine flow possibly with minimal aerodynamic losses.

Near-hub: The blade-span, H = 0.25 is at a radial location farthest from the blade-tip, hence it is the region least influenced by the complex and lossy flow near the tip gap area.

Fig. 5 shows the distribution of pressure coefficient C_p at three selected span-wise locations using all of the ensemble-

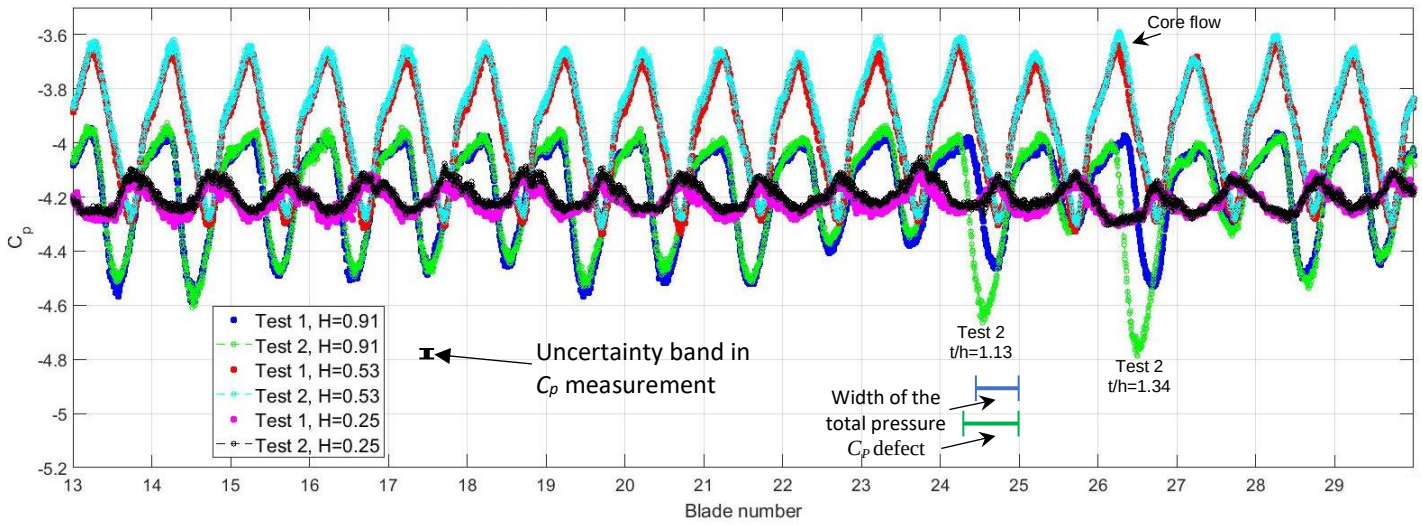

Figure 5: Ensemble-averaged total pressure coefficient at H = 0.91, H = 0.53 and H = 0.25

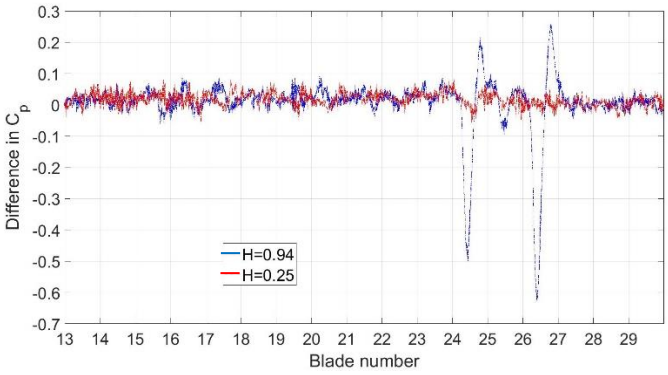

Figure 6: Difference in C_p of Test 1 and Test 2 at H=0.94 and 0.25

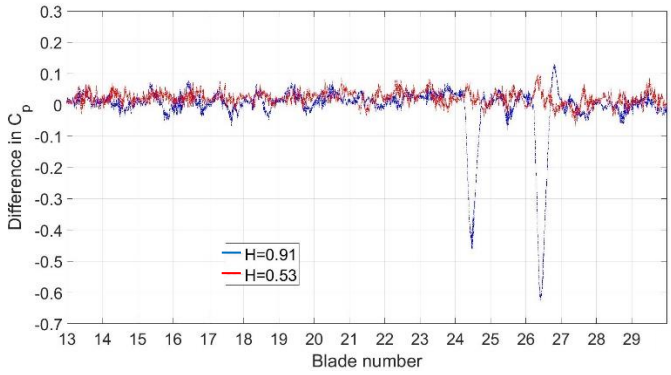

Figure 7: Difference in C_p of Test 1 and Test 2 at H=0.91 and 0.53

averaged data from blade 13 to blade 29. The region between the blades are the passages and each passage retains the corresponding blade number to its left side. The region between blade 13 and blade 14 is passage 13. The experimental uncertainty of C_p is δC_p=0.034 estimated using Kline and McClintock's [15] uncertainty analysis technique. The experimental uncertainty band associated with C_p is shown in Fig. 5.

***C_p* in the Tip Leakage Dominated Zone:** Passage 24 and 26 from Test 2 clearly shows the impact of increasing the tip clearance when compared the rest of the passages having a typical clearance value around t/h= 0.78%. There is a significant total pressure defect because of the tip vortex dominated regions with high aerodynamic loss at H = 0.91 in passages 24 and 26. An increase in the magnitude of negative C_p value indicates higher losses in this region. The coverage area of the tip leakage vortices is also indicated as the width of the C_p defect in Fig. 5. But these changes in C_p magnitude and coverage are only confined to passages 24 and 26. The C_p distribution at H = 0.91 of Test 1 closely matches (within the experimental uncertainty) with that of Test 2 for all other blade passages (except passage 24 and 26). This observation shows that there is no measurable influence of the modified blade-tip clearances on all other passages in the rotor. On increasing the tip clearance from 0.81% to 1.13% on blade 24, the peak value of negative C_p increased from -4.46 to -4.66. Similarly, for blade 26 when the tip clearance value is increased from 0.87% to 1.32%, the peak value of negative C_p at passage 26 increased from -4.52 to -4.79. On closely analyzing passages 24 and 26, the distribution of C_p at H = 0.91 remains the same for the first and last quarter of the modified passages 24 and 26. The main changes are seen only in the middle of these passages. The width of the negative C_p valley at H = 0.91 in the passage directly corresponds to the size of the leakage vortex present in the passage. Similar to the strength of the leakage vortex the size and position of the vortex also increases with the increase in tip clearance value, this can be seen by the increase in the width of the C_p valley on passages 24 and 26. This is an indication of the fact that the larger "tip vortex dominated" zone with a significant total pressure defect slightly

influences the mid-span total pressure for Test 2. The blockage effect of the larger and more lossy tip vortices of the two passages (24, 26) of Test 2 tends to increase the mean kinetic energy of the core flow as shown in Fig.5. Other data collected in AFTRF also confirms this observation.

***C_p* near Hub:** For H = 0.25, no measurable effect of the modified tip clearance can be seen as the C_p distribution from Test1 matches closely with that of Test 2. This is true for all the blade passages within the experimental uncertainty. This observation supports that the tip region changes made near the blade-tip region have not radially propagated all the way to H = 0.25. Span-wise mixing or turbulent diffusion related total pressure changes are not observable near the hub.

Difference between Test 1 and Test 2 for all passages: Fig. 6 shows the circumferential propagation effect of the local tip clearance change on all other blade passages in the rotor. This effect can be visualized by plotting the difference in C_p distribution of Test1 and Test 2 at selected blade-span-wise locations. Fig. 6 presents the difference in C_p distribution between Test1 and Test 2 for H = 0.94 and 0.25. Fig. 7 has a similar plot for blade-spans H = 0.91 and 0.53. Positive change in this difference indicates reduced aerodynamic losses in Test 2 compared to Test1 and the opposite is true for the worsened aerodynamic losses. From the Fig. 6, it can be seen that for H = 0.94 the difference in C_p fluctuates almost randomly along the zero line for passages from 13 to 23 and then from 27 to 29, indicating that there is no significant change in flow structures between Test1 and Test 2 in these passages. But in passage 24 and 26 there is a sharp increase in the negative difference in the middle of the passage indicating more aerodynamic losses in the region due to increased tip clearance value. The negative peak value of passage 26 (-0.62) is higher than that of passage 24 (-0.48). These two peak values are consistent with the artificially increased tip clearance values. In the same passages, the negative peak is followed by a positive peak indicating the aerodynamic benefit in the region. Similar to the negative peak value, the larger tip clearance has a greater positive peak value (0.25), this can be seen in passage 26. This shows that increasing the tip clearance of the blade have both positive and negative effect on the passage flow. But as can be seen from the magnitude of these positive and negative peaks, the losses generated in the passage far outweigh the losses reduced, hence resulting in net overall increased aerodynamic losses.

For H = 0.25 there is no significant change in the difference in C_p distribution as it fluctuates along the zero line for all the passages. The difference in C_p distribution of data from H = 0.91 in Fig. 7 shows a very similar trend as that of H = 0.94 data. Sudden sharp peaks can be seen only in the passages 24 and 26, and no significant changes are seen in the flow field of other passages. Both positive and negative peak values in passage 24 and 26 at H = 0.91 are slightly lower than their corresponding values at H = 0.94. For H = 0.53, a relatively small positive peak can be observed in passage 26. This indicates that the changes made near the blade tip by increasing the tip clearance are radially propagated all the way to the blade mid-span. and The influence of the blockage effect of the tip vortices effect is beneficial near the mid-span.

An important observation made from Fig. 5, 6 and 7 is that the effect of modification made to the blade tip of blade 24 and 26 are only confined to the corresponding blade passages and are not significantly spread circumferentially to other passages. This indicates that there is no strong circumferential aerodynamic interaction because of the blade tips operating with larger tip gaps.

Further Quantification of the Propagation of Disturbances to Other Passages: Quantitative analysis of the effect the modified blades on the rest of the passages can be performed by studying the span-wise distribution of pitch-wise-averaged C_p value of individual passages. The pitch-wise-averaged C_p value for a selected span-wise position in a specific passage is obtained by arithmetically averaging the C_p value at different angular locations (pitch-wise) of this passage along a complete pitch. The pitch of each passage has about 206 ensemble-averaged data points at one span-wise position (6000/29).

Removing the Possible Bias Error in *C_p* Measurement: The C_p plots presented in Fig. 5, 6 and 7 has a passage bias error associated with it. This is due to the presence of small non-negligible blade to blade geometry variations caused by the manufacturing and installation process. Most of this bias error is also due to the inherent measurement bias present in the present-day dynamic pressure transducers. The seasonal ambient temperature variations induce unpredictable zero shifts even though these transducers are said to be temperature compensated. A highly effective way of reducing this bias error is subtracting a "*reference* C_p" measured by the same transducer at a "fixed" reference point" from the actual C_p measurement obtained at any location. This difference is highly sensitive to variations imposed by the tip vortices, wakes, secondary flows, boundary layers, and the core flow in a relative way. Our current study is focused on the blade tip region modifications for aero-thermal gains. Our observations clearly show that the region near the hub is not significantly affected by the changes from the tip clearance region flow physics. The current approach uses a "*reference* C_p" value obtained from the hub region of each individual passage in the rotor.

Delta *C_p* as a Measurement Improvement: The present investigation uses a "*reference* C_p" value obtained from the hub area of the current *Cp* measurements from the DTP probe.

$$\text{Delta } C_p = C_p - (\textit{reference } C_p) \qquad \textbf{(2)}$$

Initially, the "*reference Cp*" was obtained along the pitch-line of a passage exactly at H=0.25. Although this reference value worked effectively, our experiments indicated that a regional average of the "*reference* C_p" measurement had the ability to remove more of the random fluctuations existed in our Delta C_p. Hence the blade-span data in a hub measurement

region between H =0.25 and 0.34 was chosen to calculate the reference C_p. The "reference C_p" is obtained by arithmetically averaging the pitch-wise-averaged C_p values from H = 0.25 to H = 0.34.

Delta C_p at each blade-span in a specific passage is calculated using Eq. (2). Andichamy and Camci [9] further explains in detail the usage of Delta C_p and its effectiveness in reducing the bias errors from total pressure measurements in AFTRF. Even though there is no widespread influence of one passage over another, the extent to which two passages interact can be analyzed by carefully comparing the passages using the span-wise distributions of Delta C_p.

Total Pressure Field in Passage 24: The comparison of a disturbed passage (passage 24) which has an artificially increased tip clearance (t/h=1.13%, Test 2) and its neighboring passage 23 with a t/h=0.66% is helpful in visualizing the passage to passage interactions. Fig. 8 shows the contour plot of Delta C_p distribution in passage 24 in Test1 and 2. The most efficient region in the turbine passage flow such as the core flow is indicated by the orange/red color in Fig. 8 while the blue color is assigned to indicate the least energy efficient region such as the tip leakage vortex and passage vortex. The outer arc represents 100% blade-span (H = 1.0), while the dotted arcs represents H = 0.91, H = 0.83 and H = 0.5. A detailed explanation of these contour plots is given by Andichamy and Camci [9]. The leakage vortex can be seen near H = 0.91, a region of high momentum fluid is also present circumferentially near the leakage vortex. This area is usually termed as "scraping vortex" in turbine passage flows. Fig. 8 shows that artificially increased tip clearance of blade 24 (from 0.81% to 1.13%) enlarges the size of the leakage vortex with a significant total pressure deficit in it. As the size and strength of the leakage vortex increases, it reduces the total pressure in the region, effectively increasing the losses in the passage. The mean kinetic energy of the directed motion is further dissipated into heat in this highly recirculatory flow region marked by blue and light green hues.

Pitch-wise-averaged Delta C_p in Passage 24: Fig. 9 uses the exact same data sets as the previous figure, however Delta C_p values at each span-wise position are pitch-wise-averaged. The pitch-wise-averaged Delta C_p in function of span H for Test 1 and Test 2 are compared. The green lines indicate the region of passage 24 which has lower aerodynamic losses in Test 2 than in Test 1. The regions with the higher aerodynamic losses are shown with blue lines assigned to the "degraded total pressure region". As expected, increasing the tip clearance from 0.81% to 1.13% drastically increases the losses near the tip region (H = 0.80 to 0.97, light-blue lines). But near the core of the passage, the aerodynamic losses are somewhat reduced as indicated by the green lines. This is due to the increase in the size of the tip leakage vortex. A relatively larger tip leakage vortex imposes a higher the blockage effect on the core flow. This flow blockage slightly reduces the available cross-sectional area for the core flow, which in turn slightly accelerates the core flow. Delta C_p variations from H = 0.74 to 0.56 in Fig.9 are within the

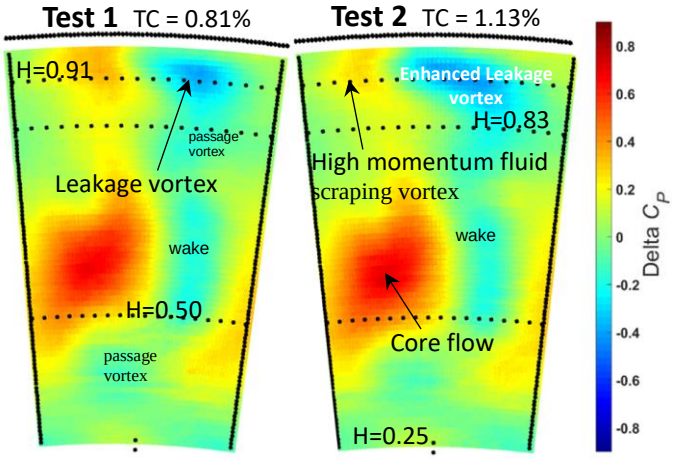

Figure 8: Delta C_p contour plot of passage 24 from Test1 and Test 2

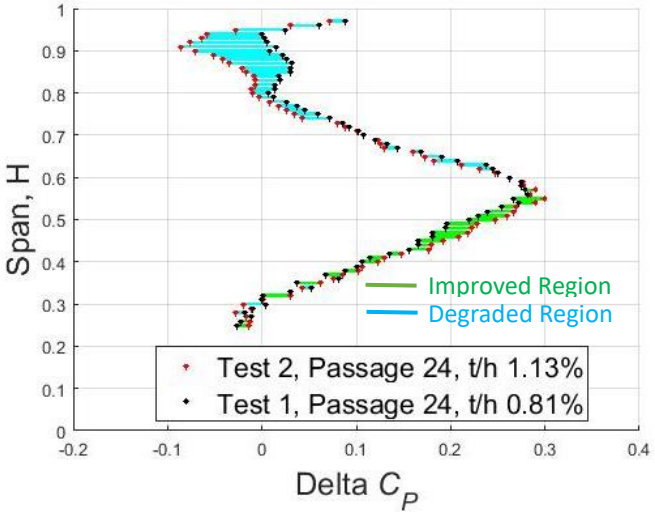

Figure 9: Span-wise distribution of pitch-wise-averaged Delta C_p of passage 24 from Test1 and test 2

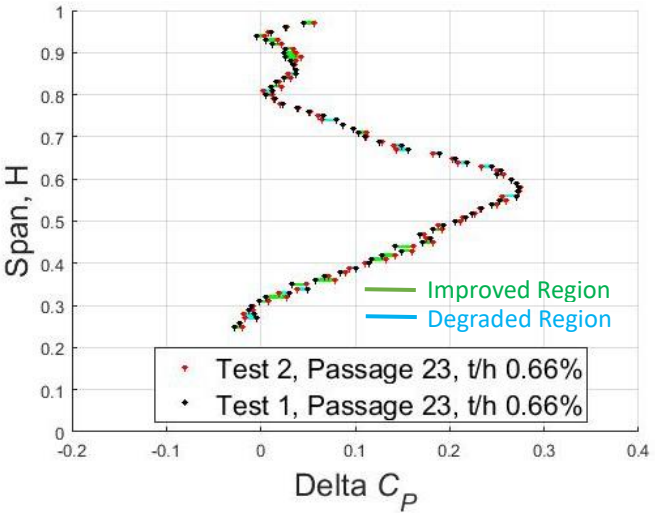

Figure 10: Span-wise distribution of pitch-wise-averaged Delta C_p of passage 23 from Test 1 and Test 2

experimental uncertainty. The same feature is also observed in the region between H = 0.25 and 0.42. Hence, these regions are assumed to be not significantly affected by the change in the tip clearance value of blade 24.

The Changes in the Immediate Suction Side Neighbor of Blade 24: In Test 2, the tip clearance value of blade 24 was artificially increased by 39.5%. Considering this large change from t/h=0.87 % to 1.13 %, it was expected that the neighboring passage 23 on the suction side of blade 24 would be significantly influenced.

The span-wise distribution of Delta C_p in the neighboring passage 23 from Test 1 and Test 2 are shown in Fig. 10. There are negligible variations near the blade tip region from H = 0.80 to 0.97. These changes are easily within the experimental uncertainty band as observed from the length of the blue and green lines. Hence, it was concluded that the artificial changes made in the tip clearance of blade 24 did not significantly affect the neighboring passage on the suction side (passage 23). This observation once again shows that there is no significant interaction between the passages in the rotational direction of the blades.

Total Pressure Field in Passage 26; Blade 26 in Test 2 was altered such that its tip clearance was artificially increased to TC=1.32% from 0.87%. This clearance increase corresponds to a 51.7% relative increase in TC. Figure 11 compares the two aerodynamic cases by comparing Delta C_p at rotor exit plane. The total pressure deficit of the leakage vortex in passage 26 increases for Test 2 when compared to Test 1. The dark blue region above H=0.83 is much larger with more total pressure deficit when compared to Test 1.

The overall losses near the blade tip region for blade 26 are further increased when compared to those of blade 24. Increasing the tip clearance also slightly benefits the core flow. This benefit can be seen at mid-span, where the total pressure for Test 2 slightly increases in the core flow when compared to Test 1. These reductions are also greater than those seen in passage 24 (Fig. 9). The changes in the region near the hub (H = 0.25 to 0.40) are within the experimental uncertainty. In passage 26, the region from H = 0.74 to H = 0.56 are clearly affected (as indicated by blue lines in Fig. 12) by the change in tip clearance of the blade 26. This is different than that of passage 24 where the effect of increased tip clearance is confined to blade tip region and core flow region. Figures 9 and 12 show that increasing the tip clearance of the blade does not only create a stronger leakage vortex in the blade tip region but also affects the flow structures in other span-wise locations of the same passage. Hence, increasing the blade tip clearance results in a measurable span-wise-mixing in the same passage.

Pitch-wise-averaged Delta C_p in Passage 26: Fig. 12 shows the pitch-wise-averaged Delta C_p distribution of passage 26 from Test 1 and Test 2. The aerodynamic loss near the tip region (H = 0.80 to 0.97) drastically increases with the specific increase in the tip clearance value. This is indicated by the blue horizontal

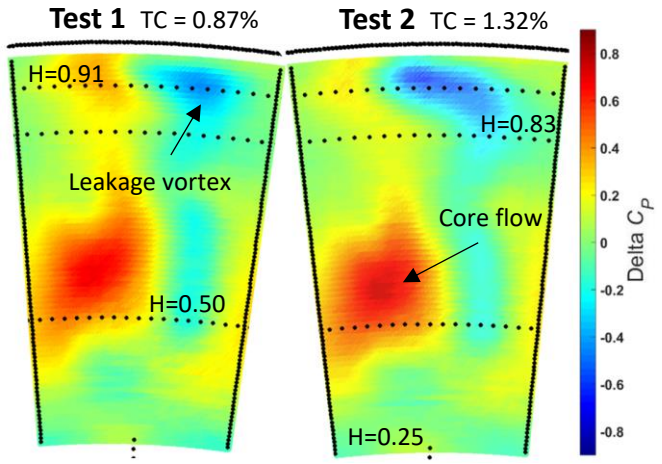

Figure 11: Delta C_p contour plot of passage 26 from Test1 and Test 2

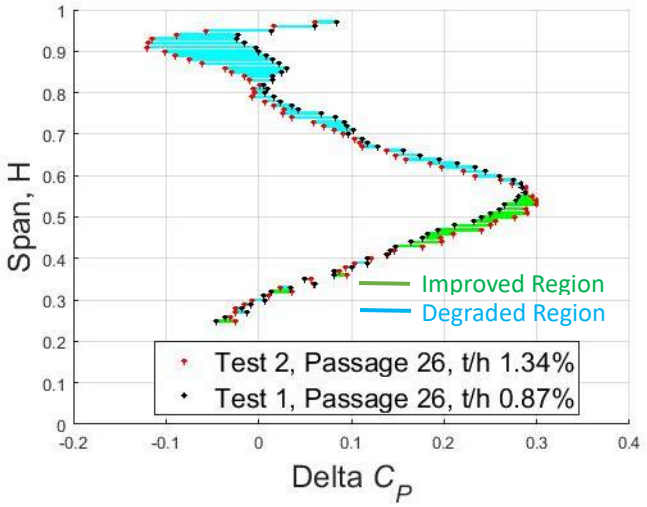

Figure 12: Span-wise distribution of pitch-wise-averaged Delta C_p of passage 26 from Test 1 and Test 2

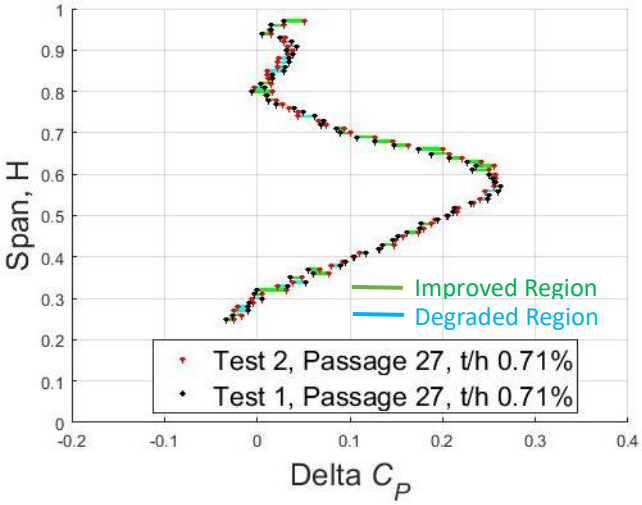

Figure 13: Span-wise distribution of pitch-wise-averaged Delta C_p of passage 27 from Test1 and Test 2

lines marking the "degraded total pressure region" in Figure 12. These losses are also greater than the losses encountered in passage 24. Similar to passage 24, the losses in the core flow of passage 26 are slightly reduced as indicated by the green horizontal lines marking the "improved total pressure region".

The Changes in the Immediate Pressure Side Passage of Blade 26: Fig. 13 shows the span-wise distribution of Delta C_p in passage 27 which is the immediate neighbor of the altered passage 26. Passage 27 is on the pressure side of passage 26 as shown in Fig.5. The results from Test 1 and Test 2 are compared. Even though there is a 51.7% increase in the tip clearance value of blade 26 for Test 2, its aerodynamic disturbance is not felt in passage 27. There are very slight changes between the Delta C_p distribution of Test1 and Test 2 as observed in Fig. 13. These changes are easily within the estimated experimental uncertainty band. The tip clearance modification made in the tip of blade 26 is not effectively propagated to the neighboring passage 27. Hence, the circumferential flow interaction between the passages in the direction opposite to the rotation of the blades is not significant.

Un-touched Passage in the Middle of the Modified Blade Passages: The un-touched Passage 25 is a suction side neighbor to the passage 24 and pressure side neighbor to the passage 26. The blades corresponding to passages 24 and 26 have both undergone artificial blade tip modifications. Hence, the mid-passage 25 needs to be evaluated for the aerodynamic influence from the two altered neighboring blade tip modifications. Fig. 14 shows the pitch-wise averaged Delta C_p distribution of passage 25 in the span-wise direction. The changes between the two plots

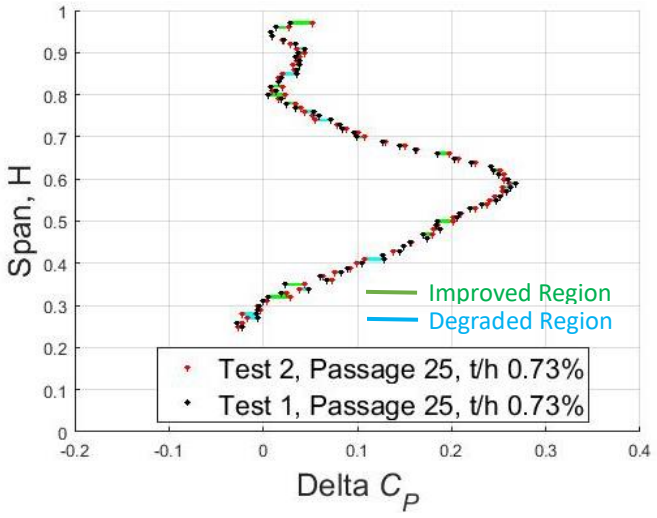

Figure 14: Span-wise distribution of pitch-wise-averaged Delta C_p of passage 25 from Test1 and test 2

for Test 1 and Test 2 are negligible and within the quoted experimental uncertainty. The passage 25 is unaffected by the artificial tip clearance changes made in both of its neighboring blades. This experimental observation confirms the results from the previous sections that the effects of the changes made in the blade tip clearances are not significantly propagated in the circumferential direction. This is true for both in the rotational and counter-rotational direction. Figure 5 clearly shows that the aerodynamic influence of the artificially altered two blades does neither propagate in the rotational direction nor counter-rotational direction over the whole rotor circumference. The passage flow influence of the altered blade tip clearances stays in their own passages with no aerodynamic influence on all other passages, including the immediately neighboring passages.

CONCLUDING REMARKS AND FUTURE WORK

The passage-to-passage aerodynamic interaction in a turbine stage is studied by modifying the tip gap of selected turbine blades and analyzing their effect on the neighboring blade passage flows.

The experiments show that the disturbances due to the altered tip clearance of one passage are not easily propagated to its neighboring turbine passages. The changes made in one of the blades in a turbine stage do not also significantly alter the aerodynamic performance of other blades. This result is particularly important for large scale turbine research rigs like AFTRF where the time accurate total pressure field is mapped in a time accurate and phase-locked manner in the presence of slight clearance variations.

The tip clearance changes made in the blade tip can be clearly seen in its own blade passage, with significant span-wise mixing. The extent of the radial propagation depends on the severity of the modifications made in the blade tip.

Even though the overall aerodynamic effect of increasing the tip clearance is negative around the tip leakage vortex, there are regions of the blade passage which benefit from this clearance increase in terms of the total pressure field. One such region is the core flow where the flow slightly accelerates in the core region due to the flow blockage effect from the leakage vortex.

The effect of modifying the blade tips by increasing their tip clearance are only seen in their own passages. All other blade passages are unaffected by this artificially increased clearance in the current experiments, within the experimental uncertainty band. This indicates that these aerodynamic changes are not effectively propagated circumferentially both in the rotational and counter-rotational direction. Even the neighboring passages of the modified blades are not significantly affected by these changes, and they behave as if no modifications have been made.

This study concludes that there is no powerful passage to passage interactions present in the turbine flow field. Hence a modification made on a turbine blade tip either deliberately or due to mechanical and thermal problems doesn't affect the performance of other unmodified blades in the same turbine rotor.

Next step in this study is to numerically analyze the complete turbine stage with all blades around the circumference for a better understanding of the fluid propagation between different blade passages due to tip clearance non-uniformity. This is a challenging task since it requires the modeling of the flow in all turbine passages simultaneously, rather than a much time efficient single-passage gridding with a circumferentially imposed periodic boundary condition.

APPENDIX

Probe Rotations: Probe incidence yaw sensitivity tests are performed at two spanwise locations (H=0.49 and H=0.93) of the rotor exit plane by Rao et al. [15]. The DTP probe in the stationary frame of reference is rotated in increments of 5^0, on either side of mean exit flow direction of α_3=25.4^0. A counterclockwise (CCW) rotation of the probe is considered positive making the probe more tangential with every increment. The rotor-averaged, and passage-averaged total pressure coefficients for a selected "test" blade, are shown in Fig. 15. The squares denote a "rotor" averaged *Cp* and the circles indicate a passage averaged *Cp* measurement.

Mid-span Yaw Sensitivity: The absolute velocity vector at mid-span is at α_3 =29.19^0, corresponding to an incidence angle of +3.79^0. The mean value of C_p at mid-span in a $\pm 10^0$ range is -3.916 and all values in this range lie within the uncertainty band of $\delta C_p = \pm$ 0.017. Mid-span experiment is represented by the solid symbols in Fig.15. Furthermore, the passage averaged coefficient for blade #21 indicates that the blade passage behaves almost identically as the rest of the rotor at mid-span. Blade # 21 is selected because of its relatively larger tip clearance compared to the rest of the blades. The influence of the larger tip clearance of blade#21 is not significant as shown by the solid symbols in Fig.15.

Tip region yaw sensitivity: At H=0.93, however, the difference between the rotor averaged and passage averaged values is considerable, due to the larger tip leakage vortex of blade#21 compared to the rest of the blades. This flow feature is consistent with the measurable difference between the passage averaged data and rotor averaged data at H=0.93. Open symbols denote the data from H=0.93. The passage averaged coefficients in the range from -20^0 to 10^0 incidence are within uncertainty limits of the mean value of *Cp* = - 4.22, computed for the range $\pm 15^0$. McCarter, et al. [17] measured lower relative tangential velocity in the tip leakage vortex region, indicating that the leakage vortex approaches the DTP at a negative incidence. The location of the maximum in the lowest distribution (open circles) of Fig.15 supports McCarter et al.'s [17] measurement. Thus, from the measurements in the range of -20^0 to 0^0 (incidence), it is possible to conclude that uncertainty in the tip vortex dominated region is within the quoted uncertainty of $\delta C_p = \pm$ 0.017, Table 3.

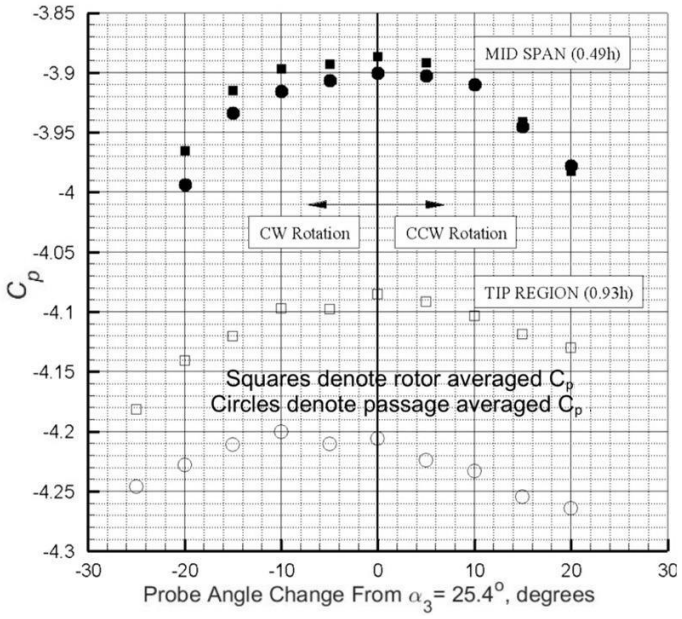

Figure 15: Dynamic Total Pressure probe DTP's Response to Incidence angle.

ACKNOWLEDGMENTS

Funding for this research from Solar Turbines, Inc. is gratefully acknowledged. In particular, we thank Mr. David Voss from Solar Turbines, Inc. for assisting us with financial support. The experimental research greatly benefited from the early contributions of Drs. J. Town, B. Gumusel, N. Rao and D. Dey especially for the measurement systems, data acquisition setup, and data reduction procedures. Many thanks to Mr. G. Khokhar for his help in automating the data post-processing system. The authors of this paper also acknowledge Mr. Benjamin Enders and Mr. K. Heller for their help in overcoming technical difficulties. Mr. H. Houtz and Mr. N. Doroschenko's support for the development and implementation of the DTP probe is acknowledged.

REFERENCES

1. Mayle R. E., Metzger D. E., 1982, "Heat Transfer at the Tip of an Unshrouded Turbine Blade", Proceedings of the 7th International Heat Transfer Conference, Munich, **3**, pp 87-92.
2. Bindon, J. P., 1987, "Pressure Distribution in the Tip Clearance Region of an Unshrouded Axial Turbine as Affecting the Problem of Tip Burnout", ASME Paper No. 87-GT-230.
3. Evans, D. M., Glezer, B., 1983, "Critical Gas Turbine Blade Tip Clearance: Heat Transfer Analysis and Experiment",

Heat and Mass Transfer in Rotating Machinery, pp. 485-497.
4. Rich, S. E., Fasching, W. A., 1982, "CF6 Jet Engine Performance Improvement - High Pressure Turbine Active Clearance Control", NASA Report CR-165556.
5. Ian N. M., 1988, "Analysis of Efficiency Sensitivity Associated with Tip Clearance in Axial Flow Compressors", International Gas Turbine and Aero-engine Congress and Exposition, **1**, Paper No. 88-GT-216.
6. Ramakrishna, P., Govardhan, M., 2010, "Study of Sweep and Induced Dihedral Effects in Subsonic Axial Flow Compressor Passages. Part II: Detailed Study of the Effects on Tip Leakage Phenomena," Int. J. Rotating Mach., 2010, Article ID 491413.
7. Andichamy, V. C., Khokhar, G. T., Camci, C., 2018, "An Experimental Study of Using Vortex Generators as Tip Leakage Flow Interrupters in an Axial Flow Turbine Stage", ASME Paper No GT2018-76994.
8. Town, J., 2015, "An Investigation of Rim Seal/Disk Cavity Flow and its Interaction with High Pressure Turbine Rotor Flows," Ph.D. Thesis, 2015d, The Pennsylvania State University.
9. Town, J., Camci, C., 2015, "A Time-Efficient Adaptive Gridding Approach and Improved Calibrations in Five Hole Probe Measurements," Int. Journal of Rotating Machinery, International J. of Rotating Machinery, Vol. 2015, Article ID 376967.
10. Andichamy, V. C., 2017, "Study of Mitigation of Turbine Blade Tip Leakage Flows using Tip Leakage Interrupter", MS Thesis, The Pennsylvania State University.
11. Lakshminarayana, B., Camci, C., Halliwell, I., Zaccaria, M., 1996, "Design, Development, and Prediction of a Turbine Research Facility to Study Rotor Stator Interaction Effects," Int. Journal of Turbo and Jet Engines, **13**, pp. 155-172.
12. Kline, S. J., McClintock, F. A., 1953, "Describing Uncertainties in Single-Sample Experiments," Mechanical Engineering, 75, pp. 3-8.
13. Camci, C., Dey, D., Kavurmacioglu, L. A., 2005, "Aerodynamics of Tip Leakage Flows Near Partial Squealer Rims in an Axial Flow Turbine Stage," ASME J. of Turbomachinery, 127, (1), 14-24**,** doi:10.1115/1.1791279.
14. Rao, N.M., Camci, C., 2004, "Injection from a Tip Trench as a Turbine Tip Desensitization Method – Part 1: Effect of Injection Mass Flow Rate," ASME paper GT2004-53256, ASME Turbo Expo Conference, Vienna, Austria.
15. Rao, N.M., Gumusel, B., Kavurmacioglu, L.A., Camci, C., 2006,"Influence of Casing Roughness on the Aerodynamic Structure of Tip Vortices in an Axial Flow Turbine ASME paper GT2006-91011 presented at the ASME International Gas Turbine Congress, Barcelona, Spain.
16. Town, J., Akturk, A., Camci, C., 2012, "Total Pressure Correction of a Sub-Miniature Five-Hole Probe in Areas of Pressure Gradients," ASME Paper No. GT2012-69280, pp. 855-861.
17. McCarter, A., 2000, "Investigation of Tip Clearance Flow Fields in a Turbine Rotor Passage," Masters Thesis, Pennsylvania State University.

